

FATIGUE CRACK GROWTH UNDER CONSTANT AND VARIABLE AMPLITUDE  
LOADING OF CAST STEEL AT ROOM AND LOW TEMPERATURE

R. I. Stephens\*, G. O. Njus\*\* and A. Fatemi\*\*

\*Professor

\*\*Research Assistant

Materials Engineering Division, The University of Iowa  
Iowa City, Iowa 52242, USA

ABSTRACT

Constant amplitude fatigue crack propagation behavior and variable amplitude fatigue crack initiation and propagation behavior were obtained at room temperature and  $-34^{\circ}\text{C}$  or  $-45^{\circ}\text{C}$  respectively, for a normalized SAE 0030 ferritic-pearlitic cast steel and a normalized, quenched and tempered C-Mn tempered martensitic cast steel. Fatigue behavior was improved at the low temperatures.

KEYWORDS

Fatigue, crack initiation, crack growth, cold temperature, cast steel, spectrum loading.

INTRODUCTION

The purpose of this research was to determine fatigue crack growth behavior of a ferritic-pearlitic cast steel and a tempered martensitic cast steel at room temperature and common operating low temperatures ( $-34^{\circ}\text{C}$  or  $-45^{\circ}\text{C}$ ) using both constant and variable amplitude loadings.  $-34^{\circ}\text{C}$  and  $-45^{\circ}\text{C}$  were chosen for the low temperature studies since these represent reasonable lower operating temperatures for many ground vehicles. Crack initiation was also analyzed for the variable amplitude loading by using a keyhole compact specimen with an as-drilled notch. This specimen-loading spectra and temperatures then simulate real-life fatigue conditions. Charpy V notch transition temperature behavior was compared with fatigue behavior and scanning electron microscopy was used to compare fatigue crack growth modes under the different test conditions.

MATERIALS AND SPECIMENS

The two cast steels were normalized SAE 0030 and a normalized, quenched and tempered C-Mn steel. The chemical composition of each is given in Table 1. Each steel was cast into blocks from a single ladle melt with a substantial riser for proper casting soundness. The blocks were then heat treated as given in Table 2. The normalized 0030 cast steel resulted in an 80 percent ferritic and 20 percent pearlitic structure. The C-Mn normalized quenched and tempered cast steel structure was tempered martensite. Both cast steels were of nominal good quality. Hardness, for a given cast steel, varied little from one block to another and within a block as measured on three orthogonal planes. Average room temperature monotonic tensile properties and hardness are given in Table 3 along with partial data at  $-34^{\circ}\text{C}$  for 0030 steel and  $-45^{\circ}\text{C}$  for C-Mn steel. These temperatures were used for low temperature tests for the steels respectively.

TABLE 1 Chemical Composition, Percent by Weight

Material	C	Mn	Si	S	P	Cr	Ni	Cu	Mo
0030	0.24	0.71	0.44	0.026	0.015	0.1	0.1	0.05	0.08
C-Mn	0.23	1.25	0.39	0.028	0.036	0.1	0.09	0.04	0.02

TABLE 2 Heat Treatment of Castings

0030 Steel	C-Mn Steel
Normalize at 900°C, 0.5 hr. Temper at 677°C, 1.5 hr.	Normalize at 900°C, 3 hr. cycle Austenitize at 900°C, 1 hr. at temp, WQ Second austenitize at 900°C, 1 hr. WQ

TABLE 3 Average Monotonic Tensile Properties

Property	0030		C-Mn	
	Room Temp.	-34°C	Room Temp.	-45°C
Ultimate strength--MPa	496		654	
Upper yield point--MPa		373	473	486
0.2% yield strength--MPa	303	325	413	401
Percent reduction in area	46		31	
Young's modulus--GPa	207	209	208	208
Brinell hardness	137		174	

Charpy V notch energy values obtained for each cast steel are shown in Fig. 1. For the 0030 steel, room temperature is in the upper transition region, while -34°C is in the lower transition or lower shelf region. For the C-Mn cast steel, room temperature is in the upper shelf region, while -45°C is in the lower transition region. Percent crystalline fracture surface and lateral expansion temperature transitions were in agreement with the energy transitions. Thus under Charpy V notch impact conditions, both steels behaved in a ductile manner at room temperature and in a brittle manner at the cold temperatures used for the fatigue studies.

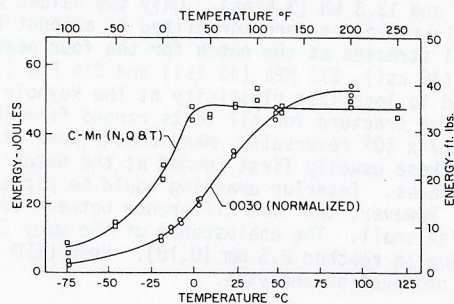


Fig. 1 Charpy V notch impact energy.

Compact-type chevron specimens used for constant amplitude fatigue crack growth tests and 4.8-mm (3/16-in.) dia. keyhole specimens used to study both crack initiation and crack growth under variable amplitude loading are shown in Fig. 2. H/W ratios were 0.49 for the 0030 steel and 0.60 for the C-Mn steel. The three-hole configuration was used to allow compression with a "monoball" gripping system that assured axial ram loading. An 89-kN (20-kip) closed-loop electrohydraulic test system was used for all fatigue tests. Nominal specimen thickness was 8.3 mm (0.324 in.). Specimens were machined from the cast blocks. The keyhole notches were formed by drilling only, without any subsequent operation on the hole.

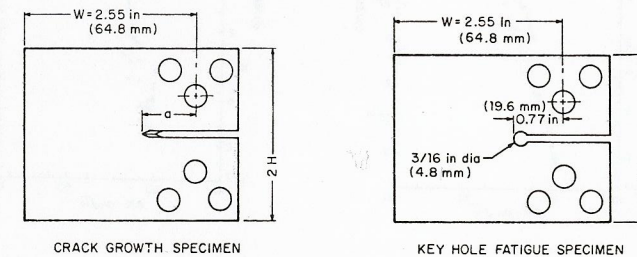


Fig. 2 Test specimens

## CONSTANT AMPLITUDE FATIGUE CRACK GROWTH

These crack growth tests were conducted with the compact chevron specimens in load control. The ASTM standard test practice (E647) for constant-load-amplitude fatigue crack growth rates above  $10^{-8}$  m/cycle was followed. Crack extension was monitored with a 33X traveling telescope with a least reading of 0.01 mm. Tests were performed with several initial stress intensity ranges to obtain crack growth rates from less than  $10^{-8}$  m/cycles to about  $10^{-5}$  m/cycle. This region often represents the straight line portion of the log-log sigmoidal-shaped  $da/dN$  versus  $\Delta K$  curve. Test frequencies varied from 10 to 35 Hz depending upon load ratio, initial stress intensity factor range, and crack length. The cold temperature tests were performed in an automated CO<sub>2</sub> cold temperature chamber.

The results of a versus N were reduced to  $da/dN$  versus  $\Delta K$  by using a second-order incremented polynomial as suggested in the ASTM E647 standard.  $da/dN$  versus  $\Delta K$  for 0030 steel with  $R \approx 0$  and -1 at room temperature and -34°C is shown in Figs. 3 and 4 while Figs. 5 and 6 give the data for C-Mn steel with  $R \approx 0$  and +1/2 respectively for room temperature and -45°C. The data scatter for 0030 steel with  $R = -1$  at low temperature is substantially greater due to difficulties with monitoring crack length under these conditions. This difficulty was the main reason for not testing the C-Mn steel at  $R = -1$ . Despite the scatter, it is evident that fatigue crack growth rates at the lower temperatures are about equal to or lower than room temperature rates. Some slight crossing occurred at the higher rates for C-Mn steel with  $R \approx 0$ . Thus in general, these typical low operating temperatures were not detrimental to constant amplitude fatigue crack growth behavior, despite the fact the low temperatures were in the lower shelf or lower Charpy V notch transition region.

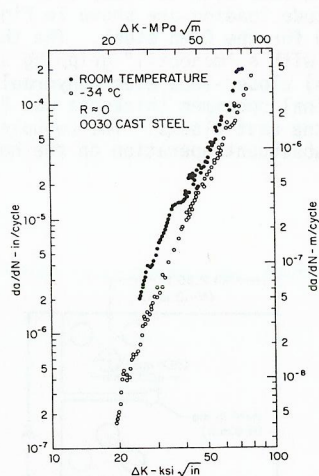


Fig. 3 Constant amplitude fatigue crack growth  $R \approx 0$ , SAE 0030.

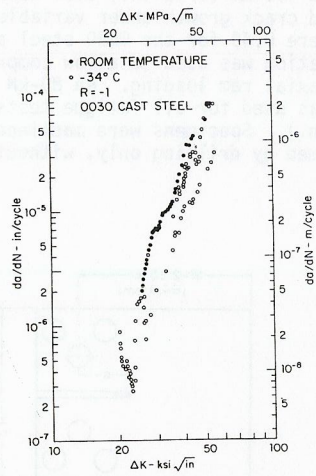


Fig. 4 Constant amplitude fatigue crack growth  $R = -1$ , SAE 0030.

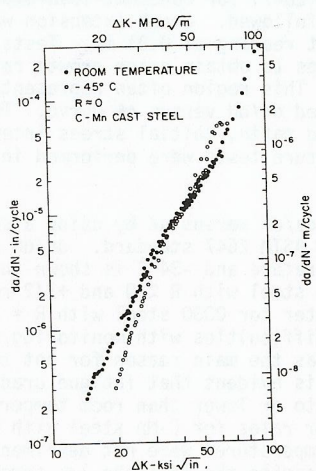


Fig. 5 Constant amplitude fatigue crack growth  $R \approx 0$ , C-Mn steel.

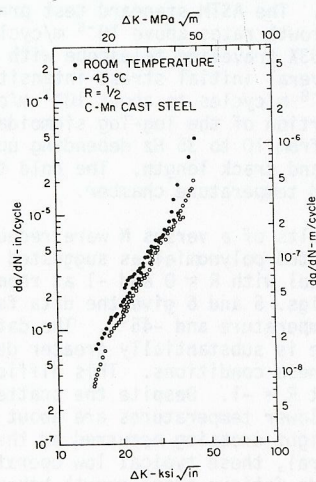


Fig. 6 Constant amplitude fatigue crack growth  $R = +1/2$ , C-Mn steel.

VARIABLE AMPLITUDE FATIGUE

The SAE transmission history labeled "T/H" shown in Fig. 7(a) plus a modification of this history shown in Fig. 7(b) labeled "mod T/H" was used in conjunction with the keyhole specimen of Fig. 2 for the variable amplitude loading. The keyhole has a stress concentration factor of about 3.65 as interpolated from work by Wilson (1974) and Neal, Zachary, and Burger (1978). The T/H history has 1708 reversals in one block while the mod T/H history has 1692 reversals. The difference is due to the truncation of all the compressive loadings. An automated profiler was used in conjunction with the test system in load control to apply the histories to the keyhole specimen. The block history was repeated until specimen fracture. Fatigue crack initiation and crack growth were monitored with the same optical system used with the constant amplitude crack growth specimens plus an electropotential system to better aid in crack initiation at the notch. Fatigue crack initiation was quantitatively defined as the first visible surface crack length of  $\Delta a = 0.25$  mm (0.01 in.), which could be observed with both the optical and electropotential system. A crack length of  $\Delta a = 2.5$  mm (0.1 in.) was also specifically monitored since this value was previously selected by the SAE Fatigue Design and Evaluation Committee as a limiting value of crack initiation used with notch strain analysis prediction methods (Wetzel, 1977). The T/H and mod T/H histories were applied at 12 Hz.

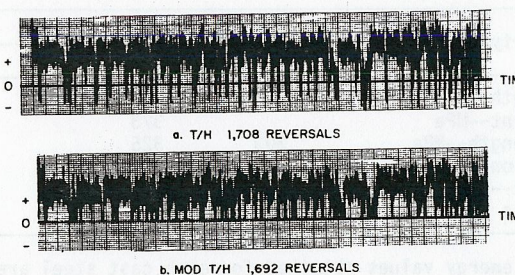


Fig. 7 Variable amplitude load spectra T/H and mod T/H.

The T/H and mod T/H histories begin and end with zero load. The first and last load in each block has the same peak value  $P_{max}$ . Three or four values of  $P_{max}$  were chosen for the T/H history which were 22.2 kN (5 kips), 17.8 kN (4 kips), 15.6 kN (3.5 kips) and 13.3 kN (3 kips). Only two values were used with the mod T/H history. These values were normalized to account for small variations in thickness. Nominal stresses at the notch for the four peak loads were 393 MPa (57 ksi), 314 MPa (46 ksi), 275 MPa (40 ksi) and 236 MPa (34 ksi). All specimens were thus subjected to localized plasticity at the keyhole notch on the first loading. Total blocks to fracture for all tests ranged from 55 to 1590, equivalent to about  $8 \times 10^4$  to  $2.7 \times 10^6$  reversals. Many cracks were often initiated at the keyhole notch edge. These usually first formed at the keyhole interior and then spread to the outside surfaces. Interior cracking could be picked up by the electrical potential system. However, the time difference between interior and surface crack initiation was quite small. The coalescence of the many interior cracks was often complete by the time  $\Delta a$  reached 2.5 mm (0.10). Here LEFM principals can definitely be used for crack propagation analysis.

The results of the variable amplitude tests for the 0030 steel with both load histories at room temperature (solid columns) and -34°C (dotted columns) are given in the form of a bar chart in Fig. 8. The results for C-Mn steel at room temperature (solid columns) and -45°C (dotted columns) are shown in Fig. 9. Each column represents the results from only one specimen. A key is given in each figure to denote the number of blocks to crack initiation ( $\Delta a = 0.25$  mm), the number of blocks to  $\Delta a = 2.5$  mm, and the number of blocks to fracture. Each  $P_{max}$  load level is indicated. Very little scatter existed for a given test condition. The number of blocks within the three criteria regions designated in Figs. 8 and 9 for a given specimen ranged from 20 to 60 percent to initiate the crack ( $\Delta a = 0.25$  mm), and then 15 to 40 percent to grow the crack to  $\Delta a = 2.5$  mm, followed by 20 to 60 percent to grow the crack to fracture. Thus all three regions, in general, significantly contributed to the total fatigue life at all temperatures considered. The cold temperature total fatigue life and fatigue crack growth life was always better than that at room temperature by 20 to 120 percent. Crack initiation life increased from zero to 100 percent at the cold temperatures. Thus the cold temperatures enhanced both fatigue crack initiation life and crack propagation life. The latter was apparent for both constant amplitude and variable amplitude loading.

Eliminating the compression for both room temperature and cold temperature increased fatigue crack initiation life between 100 and 600 percent and 10 to 200 percent for crack propagation. Thus under variable amplitude loading compression was more detrimental to fatigue crack initiation than to crack propagation.

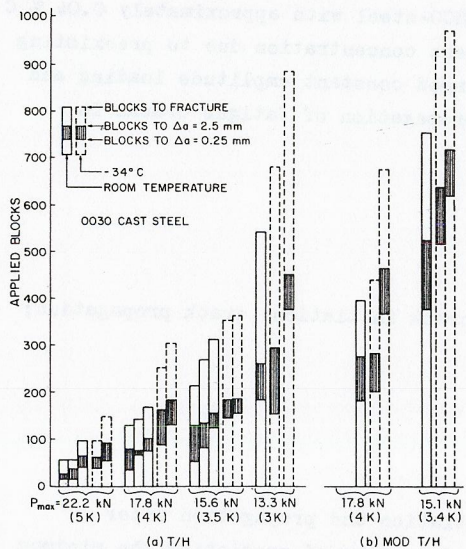


Fig. 8 Blocks to specific crack lengths and fracture for T/H and mod T/H load histories, SAE 0030 steel.

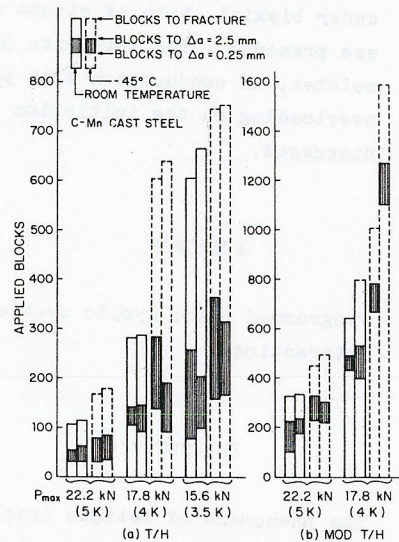


Fig. 9 Blocks to specific crack lengths and fracture for T/H and mod T/H load histories, C-Mn steel.

DISCUSSION OF RESULTS

Even though the low temperature fatigue tests were run in the lower shelf or lower transition Charpy V notch region, the low temperature fatigue properties were better than at room temperature which was in the upper shelf or upper transition Charpy V notch region. Scanning electron fractographs of the different test conditions revealed little differences in the fracture surface morphology at room temperature and low temperature for both cast steels. Typical fracture surfaces are shown in Fig. 10 for the two steels at room temperature and low temperature for the T/H history. Cracks grew from bottom to top in the photos. Fatigue striations were found under all test conditions, except fewer were found for the tempered martensitic C-Mn steel. More surface damage from crack closure could be found for the T/H history which includes substantial compressive loadings. Fatigue cracks were transcrystalline and many secondary cracks occurred for all test conditions as shown in Fig. 10. The fatigue crack propagation mode was ductile under all test conditions. Comparison of final crack lengths revealed little differences occurred at room or low temperatures for a given material and loading. Thus fracture toughness was not substantially affected by the low temperature under these fatigue conditions.

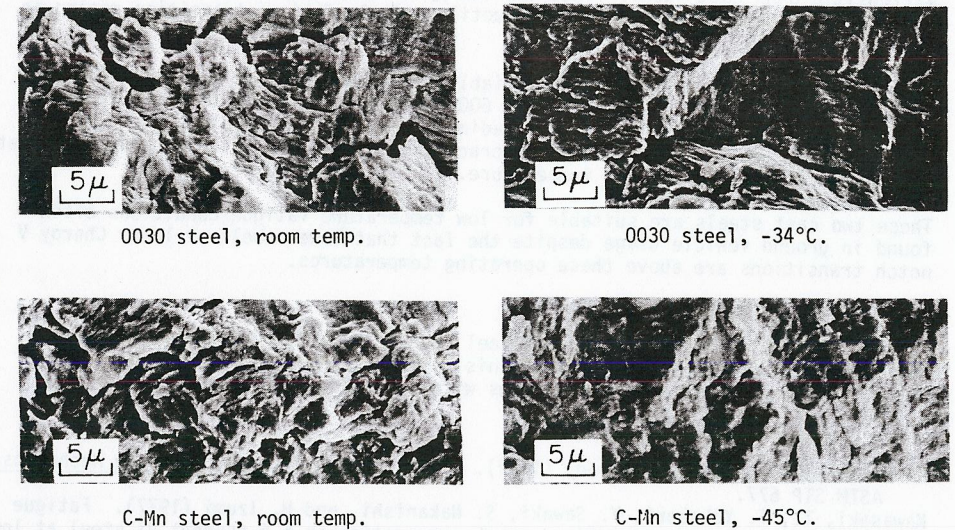


Fig. 10 SEM fractographs from T/H history.

The lack of any change in fatigue modes at the low temperature indicates the ductile-brittle transition region obtained from Charpy V notch tests is not indicative of a ductile-brittle transition in fatigue. A ductile-brittle fatigue transition region which can occur in steels has been found by others, for example, Gerberich and Moody (1979), Tobler and Reed (1977), and Kawasaki and others (1977) and summarized by Stephens, Chung and Glinka (1979), to be below the Charpy V notch transition. This can be attributed to several aspects including strain rate, size effect and the fatigue process. Additional tests at -60°C using only the T/H history and the 17.8 kN (4 kip)  $P_{max}$  loading indicated fatigue behavior was still not worse than at room temperature for either cast steel. Thus a brittle-ductile

fatigue transition region for these two cast steels is well below the normal ground vehicle operating temperatures.

#### SUMMARY AND CONCLUSIONS

Fatigue crack initiation and propagation lives in the 0030 and C-Mn cast steels were better at the low temperatures than at room temperature for the two variable amplitude load histories. Fatigue crack propagation rates at low temperatures under constant load amplitude conditions were equal to or lower than room temperature rates. Final fatigue crack lengths for a given material and loading were essentially unaffected by the low temperatures. Fatigue crack initiation life, crack propagation life and total life were increased up to about 100 percent or more at the low temperatures. Thus the low temperatures enhanced both crack initiation and crack propagation lives even though low temperature tests were performed in the lower shelf or lower Charpy V notch transition regions.

Fractographic SEM studies indicated little difference between the room temperature and low temperature fatigue crack growth modes. Striations and ductile tearing were evident at all temperatures with fewer striations being found in the tempered martensitic C-Mn cast steel. Thus the Charpy V notch temperature transition region is not an indication of the possible ductile-brittle fatigue transition region in these cast steels.

Eliminating the compression in the variable amplitude loadings increased fatigue crack initiation lives between 100 and 600 percent and between 10 and 250 percent for crack propagation. Compression loadings under variable amplitude conditions were thus more detrimental to fatigue crack initiation than to crack propagation at both room temperature and low temperature.

These two cast steels are suitable for low temperature fatigue conditions often found in ground vehicle usage despite the fact that lower shelf or lower Charpy V notch transitions are above these operating temperatures.

#### ACKNOWLEDGEMENT

The authors would like to thank the Steel Founder's Society of America and Deere and Company for financial support of this research. Also Mr. C. M. Wang and Mr. B. Boardman for their contributions with the scanning electron microscopy.

#### REFERENCES

- Gerberich, W. W. and M. R. Moody (1979). In C. W. Smith (Ed.), Fracture Mechanics, ASTM STP 677.
- Kawasaki, T., T. Yokobori, Y. Sawaki, S. Nakanishi, and H. Izumi (1977). Fatigue fracture toughness and fatigue crack propagation in 5.5 percent Ni steel at low temperatures. In D. M. R. Taplin (Ed.), Fracture, ICF-4, Vol. 3.
- Neal, S., L. W. Zachary, and C. P. Burger (1978). Three-dimensional stress analysis of the SAE keyhole fatigue specimen, SAE paper no. 780104.
- Stephens, R. I., J. H. Chung, and G. Glinka (1979). Low temperature fatigue behavior of steels - A review, SAE paper no. 790517.
- Tobler, R. L., and R. P. Reed (1977). Fatigue crack growth resistance of structural alloys at cryogenic temperatures. Cryogenic Engineering Conf./Int. Cryogenics Materials Conf., U. of Boulder, Colorado.
- Wetzel, R. M., Editor (1977). Fatigue under Complex Loading: Analyses and Experiments, SAE, Warrendale, Pennsylvania.
- Wilson, W. K. (1974). Elastic-plastic analysis of blunt notched CT specimens and applications. J. of Pressure Vessel and Technology, ASME, Vol. 96, No. 4.